

A Conformation-Dependent Neutralizing Monoclonal Antibody Specifically Targeting Receptor-Binding Domain in MERS-CoV Spike Protein

Short title: Neutralizing antibody targeting MERS-CoV S protein RBD

Lanying Du^{a¶}, Guangyu Zhao^{b¶}, Yang Yang^{c¶}, Hongjie Qiu^b, Lili Wang^a, Zhihua Kou^b, Xinrong
Tao^d, Hong Yu^b, Shihui Sun^b, Chien-Te K Tseng^d, Shibo Jiang^{a,c}, Fang Li^{c#}, Yusen Zhou^{b#}

^aLindsley F. Kimball Research Institute, New York Blood Center, New York, NY, USA

^bState Key Laboratory of Pathogen and Biosecurity, Beijing Institute of Microbiology and
Epidemiology, Beijing, China

^cDepartment of Pharmacology, University of Minnesota Medical School, Minneapolis, Minnesota,
USA

^dDepartment of Microbiology and Immunology, and Center for Biodefense and Emerging Disease,
University of Texas Medical Branch, Galveston, Texas, USA

^eKey Laboratory of Medical Molecular Virology of Ministries of Education and Health, Shanghai
Medical College and Institute of Medical Microbiology, Fudan University, Shanghai, China

[¶]These authors contributed equally to this work.

[#]Correspondence. E-mail: lifang@umn.edu (F. Li); yszhou@bmi.ac.cn (Y. Zhou).

Word count Abstract 138 words; text 3,170 words

21 **ABSTRACT**

22 Prophylactic and therapeutic strategies are urgently needed to combat infections caused by the
 23 newly emerged Middle East respiratory syndrome coronavirus (MERS-CoV). Here we have
 24 developed a neutralizing monoclonal antibody (mAb), designated Mersmab1, which potently
 25 blocks MERS-CoV entry into human cells. Biochemical assays reveal that Mersmab1 specifically
 26 binds to the receptor-binding domain (RBD) of the MERS-CoV spike protein, and thereby
 27 competitively blocks the binding of the RBD to its cellular receptor dipeptidyl peptidase 4 (DPP4).
 28 Furthermore, alanine scanning of the RBD has identified several residues at the DPP4-binding
 29 surface that serve as neutralizing epitopes for Mersmab1. These results suggest that if humanized,
 30 Mersmab1 can potentially function as a therapeutic antibody for treating and preventing
 31 MERS-CoV infections. Additionally, Mersmab1 may facilitate studies on the conformation and
 32 antigenicity of MERS-CoV RBD and thus will guide rational design of MERS-CoV subunit
 33 vaccines.

34 **Key words:** MERS; MERS-CoV; spike protein; receptor-binding domain; monoclonal antibodies;
 35 neutralizing eptiopes; immunotherapeutics

36

37 **IMPORTANCE**

38 MERS coronavirus (MERS-CoV) is spreading in the human population and causing severe
39 respiratory diseases with over 40% fatality. No vaccine is currently available to prevent
40 MERS-CoV infections. Here, we have produced a neutralizing monoclonal antibody with the
41 capacity to effectively block MERS-CoV entry into permissive human cells. If humanized, this
42 antibody may be used as a prophylactic and therapeutic agent against MERS-CoV infections.
43 Specifically, when given to a person (e.g., a patient's family member or a healthcare worker),
44 either before or after exposure to MERS-CoV, the humanized antibody may prevent or inhibit
45 MERS-CoV infection, thereby stopping the spread of MERS-CoV in humans. This antibody can
46 also serve as a useful tool to guide the design of effective MERS-CoV vaccines.

47

48

49

50 INTRODUCTION

51 The newly emerged Middle East respiratory syndrome coronavirus (MERS-CoV) causes
52 severe pneumonia and renal failure in infected patients and has led to 206 laboratory-confirmed
53 MERS cases, including 86 deaths (a case fatality rate of ~42%) (1)
54 (http://www.who.int/csr/don/2014_03_27_mers/en/). The symptoms caused by MERS-CoV
55 infection are similar to those caused by the severe acute respiratory syndrome coronavirus
56 (SARS-CoV), the latter of which led to over 8000 infections and a fatality rate of ~10% during the
57 2002-2003 SARS epidemic (2, 3). While no new SARS-CoV case has been reported since 2005
58 (4), the number of reported cases for MERS-CoV infections is still rising. Despite the high fatality
59 rate of MERS-CoV and its ongoing spread in the human population (5, 6), no vaccine or antiviral
60 therapeutic is currently available to combat MERS-CoV infections. Therefore, development of
61 strategies to prevent and treat MERS-CoV infections is urgent. This study aims to develop such a
62 strategy.

63 MERS-CoV and SARS-CoV both belong to the β -genus of the coronavirus family (1, 7).
64 Coronaviruses are enveloped and positive-stranded RNA viruses. The entry of coronavirus into

65 host cells is mediated by a viral-envelope-anchored spike protein (8-10). The spike protein
 66 contains a receptor-binding subunit S1 and a membrane-fusion subunit S2. As a first step of viral
 67 entry, a defined receptor-binding domain (RBD) in the S1 subunit binds to a host receptor on the
 68 cell surface (4, 11, 12). The host receptors for MERS-CoV and SARS-CoV are dipeptidyl
 69 peptidase 4 (DPP4) and angiotensin-converting enzymes 2 (ACE2), respectively (13, 14).
 70 Structural studies show that the RBDs of MERS-CoV and SARS-CoV comprised of a core
 71 structure and a receptor-binding motif (RBM) (12, 15-18). Whereas the core structures of these
 72 two RBDs are highly similar, their RBMs are significantly different, leading to different
 73 receptor-binding specificities. Following receptor binding, the S2 subunit of the spike protein
 74 undergoes a dramatic conformational change to fuse the viral and host membranes, allowing
 75 coronaviruses to penetrate cell membranes (10, 19). This knowledge has paved the way for
 76 possible human intervention to block the entry of coronaviruses into host cells.

77 Viral entry into host cells may be targeted in various ways (4). Vaccination remains one of the
 78 most effective approaches to control viral infections (20). In fact, both MERS-CoV and
 79 SARS-CoV RBDs can elicit strong neutralizing immune responses, and hence potentially function

80 as subunit vaccines (21-23). However, vaccines generally cannot provide immediate prophylactic
 81 protection or be used to treat ongoing viral infections. Instead, passive immunotherapeutics using
 82 neutralizing monoclonal antibodies (mAbs) have recently emerged as a powerful tool to provide
 83 prophylactic and therapeutic protections against viral infections (24, 25). For example, a potent
 84 therapeutic mAb, Palivizumab, is currently used clinically to prevent and treat respiratory
 85 syncytial virus (RSV) infection in infants (26). In addition, several mAbs have been developed to
 86 combat SARS-CoV and influenza virus infections (24, 27). These therapeutic mAbs target the
 87 viral surface spike glycoproteins and block either the receptor binding or the membrane fusion
 88 step (28-30). These studies suggest that therapeutic mAbs may be a promising approach to prevent
 89 and treat MERS-CoV infections.

90 In this study, we report the generation of a novel monoclonal antibody, Mermab1, which
 91 targets the MERS-CoV RBD and blocks MERS-CoV entry into host cells. We have also
 92 characterized the neutralizing potency, RBD-binding specificity, and recognizing epitopes of
 93 Mersmab1, and discussed its potential use in controlling MERS-CoV infections.

94

95

96 **MATERIALS AND METHODS**

97 **Ethics Statement.** Female BALB/c mice at the age of 6-8 weeks old were used for mAb
 98 production. The animal studies were carried out in strict accordance with the recommendations in
 99 the Guide for the Care and Use of Laboratory Animals of the U.S. National Institutes of Health
 100 and of the State Key Laboratory of Pathogen and Biosecurity at the Beijing Institute of
 101 Microbiology and Epidemiology of China. The animal protocol was approved by the Committee
 102 on the Ethics of Animal Experiments of the Beijing Institute of Microbiology and Epidemiology
 103 (Permit Number: PMB13.02).

104

105 **Expression and purification of recombinant proteins.** Recombinant MERS-CoV S1 or S2
 106 protein fragments (strain EMC, GenBank ID: AFS88936.1) were expressed and purified using a
 107 protocol as previously described (31). Briefly, the protein fragments were fused with either a
 108 C-terminal Fc tag of human IgG or a C-terminal His₆ tag, and were transiently expressed in 293T
 109 cells. The protein fragments were harvested from the cell culture supernatants, and purified using

110 Protein A Sepharose Beads (GE Healthcare, NJ) (for Fc-tagged proteins) or Ni-NTA Superflow
111 (Qiagen, CA) (for His₆-tagged proteins).

112 Recombinant human DPP4 ectodomain (residues 39–766) was expressed and purified using a
113 protocol as previously described for other coronavirus receptor proteins (16). Briefly, human
114 DPP4 ectodomain with a C-terminal His₆ tag was expressed in insect cells using the bac-to-bac
115 system (Life Technologies, CA). The protein was harvested from the cell culture supernatants, and
116 purified sequentially on Ni-NTA column and Superdex200 size exclusion column (GE
117 Healthcare).

118

119 **Generation of anti-MERS-CoV mAbs.** Anti-MERS-CoV mAbs were generated using a protocol
120 as previously described (24). Briefly, mice were immunized subcutaneously three times with
121 MERS-CoV S1 subunit (residues 18–725) containing a C-terminal human IgG Fc tag (S1-Fc, 10
122 µg/mouse). Aluminum was used as an adjuvant (InvivoGen, CA). Mice were sacrificed 10 days
123 after the last immunization, and their splenocytes were fused with mouse myeloma cells. Positive
124 hybridomas were screened by ELISA using a recombinant MERS-CoV S1 containing an

125 C-terminal His₆ tag (S1-His) (32). Positive cells were expanded and subcloned to generate stable
126 hybridoma cell lines. The mAbs were purified from ascites using Protein A and G Sepharose 4
127 Fast Flow (GE Healthcare). To obtain the Fab region of mAbs, mAbs were digested using papain
128 (Sigma, MO) and the resulting Fabs were purified as previously described (24).

129

130 **Inhibition of MERS-CoV-spike-mediated pseudovirus entry into target cells.** Entry of
131 MERS-CoV-spike-mediated pseudoviruses into Huh-7 cells was inhibited by mAbs using a
132 protocol as previously described (33). Briefly, 293T cells were co-transfected with a plasmid
133 encoding Env-defective and luciferase-expressing HIV-1 genome (pNL4-3.luc.RE) and a plasmid
134 expressing MERS-CoV spike protein. The produced pseudovirus particles were harvested 72 h
135 post-transfection from the cell culture supernatant. The pseudovirus particles were subsequently
136 incubated with the mAbs at 37°C for 1 h. The above mixture was then added to DPP4-expressing
137 Huh-7 cells, which had been pre-plated in 96-well tissue culture plates (10⁴/well) 6 h before
138 infection. After another 72 h, the cells were lysed with cell lysis buffer (Promega, WI). Lysates

139 were transferred into 96-well luminometer plates, and the luciferase activity was determined using
140 an Infinite M1000 luminometer (Tecan, CA).

141

142 **MERS-CoV neutralization assay.** The efficacy of mAbs in neutralizing MERS-CoV infection in
143 DPP4-expressing Vero E6 or Calu-3 cells was determined using a micro-neutralization assay as
144 previously described (22, 34). For neutralizing assay using Vero E6 cells, each of the serially
145 diluted anti-MERS-CoV mAbs was incubated with 0.1 MOI MERS-CoV (strain EMC) at 37°C
146 for 1 h. The mixture was then incubated with Vero E6 cells at 37°C for 72 h. The inhibitory
147 capacity of each of the mAbs was assessed by determining the presence or absence of virus-induced
148 cytopathic effect (CPE). The 50% neutralization dose (ND₅₀) was defined as the concentration of
149 the mAb that completely inhibited virus-induced CPE in at least 50% of the wells (35).

150 Anti-SARS-CoV-RBD mAb, 33G4, was used as a control (27). For neutralizing assay using
151 Calu-3 cells, the mixture of Mersmab1 and virus was incubated with Calu-3 cells at 37°C for 24 h.

152 The efficacy of Mersmab1 in attenuating MERS-CoV-induced CPE was observed under an

153 inverted microscope (Olympus 1X51). Levels of CPE were scored as follows: CPE0 (no CPE),
154 CPE1 (5–10%), CPE2 (10–25%), CPE3 (25–50%), and CPE4 (>50%).

155

156 **AlphaScreen assay.** AlphaScreen assay was performed to detect the binding between Mersmab1
157 and MERS-CoV RBD. MERS-CoV RBD (residues 367–588) containing a C-terminal His₆ tag (15)
158 was incubated with Mersmab1 at room temperature for 1 h. AlphaScreen Nickel Chelate Donor
159 Beads and AlphaScreen protein A acceptor beads (5 µg/ml each) (PerkinElmer, Massachusetts)
160 were then added to the mixture. After incubation at room temperature for 1 h, the AlphaScreen
161 signal was detected using an EnSpire plate reader (PerkinElmer).

162 The AlphaScreen assay was also used to detect whether Mersmab1 inhibited the binding
163 between MERS-CoV RBD and recombinant DPP4. To this end, MERS-CoV RBD-Fc (residues
164 377–588 containing a C-terminal Fc tag) was mixed with recombinant DPP4 in the presence of
165 Mersmab1-Fab. The remaining AlphaScreen assay was carried out as described above.

166

167 **Flow cytometry.** Flow cytometry was performed to detect whether Mersmab1 inhibited the
 168 binding between MERS-CoV RBD and cell-surface DPP4 (22). Briefly, DPP4-expressing Huh-7
 169 cells were incubated with MERS-CoV RBD-Fc (0.5 µg/ml) in the presence or absence of
 170 Mersmab1 at various concentrations at room temperature for 30 min. DyLight-488-labeled goat
 171 anti-human IgG antibody was then added. After incubation at room temperature for another 30
 172 min, the flow cytometry signal was analyzed.

173

174 **ELISA.** Binding of Mersmab1 to different regions of the MERS-CoV spike or mutant
 175 MERS-CoV RBD proteins was detected by ELISA (24). Briefly, ELISA plates were coated
 176 overnight at 4°C with recombinant proteins (1 µg/ml) corresponding to various lengths of the
 177 MERS-CoV spike or mutant RBD proteins. After blocking at 37°C for 2 h, Mersmab1 or
 178 SARS-CoV 33G4 mAb control was added to the plates. After incubation at 37°C for 1 h, one of
 179 the following reagents was added to the plates: horseradish peroxidase (HRP)-conjugated
 180 anti-mouse IgG (1:3,000, GE Healthcare), IgG1 (1:2,000), IgG2a (1:5,000), IgG2b (1:2,000) and
 181 IgG3 (1:2,000) (Invitrogen, CA). After incubation for another hour at 37°C, the substrate

182 3,3',5,5'-tetramethylbenzidine (TMB) (Life Technologies) was added. The reaction continued for
183 10 min and was subsequently stopped by adding 25 μ l 1N H₂SO₄. The ELISA signal was
184 measured using ELISA plate reader (Tecan).

185 To detect the binding between Mersmab1 and denatured MERS-CoV spike protein fragments,
186 ELISA plates were coated with recombinant spike protein fragments (1 μ g/ml) at 4°C overnight,
187 and then treated with Dithiothreitol (DTT, 10 mM, Sigma) at 37°C for 1 h, followed by addition
188 of Iodoacetamide (50 mM, Sigma) at 37°C for 1 h to stop the reaction (24). After three washes,
189 regular ELISA was performed as described above.

190

191 **RESULTS**

192 **Generation of Mersmab1 that potently neutralizes MERS-CoV cell entry**

193 To generate mAbs capable of neutralizing MERS-CoV infection, mice were immunized with
194 recombinant MERS-CoV S1 fused to a C-terminal Fc tag (S1-Fc). Subsequently, stable hybridoma
195 cell lines were generated for screening of positive clones using ELISA. These selected clones not
196 only reacted to recombinant MERS-CoV S1-Fc protein, but also to recombinant MERS-CoV S1

197 containing a C-terminal His₆ tag (S1-His₆). The latter step aimed to eliminate the selection of the
198 clones targeting the Fc fusion tag, ensuring that the generated mAbs specifically targeted the
199 MERS-CoV S1 region.

200 The selected anti-MERS-CoV mAbs were tested for their inhibition of pseudovirus entry
201 mediated by MERS-CoV spike protein and for their neutralizing activity against live MERS-CoV
202 infection in DPP4-expressing Vero E6 cells. Among the four selected mAbs (designated
203 Mersmab1, Mersmab2, Mersmab3 and Mersmab10), Mersmab1, demonstrated the most potent
204 anti-MERS-CoV activities (Fig. 1A and 1B). Not only was Mersmab1 highly effective in blocking
205 the entry of MERS-CoV-spike-mediated pseudoviruses into DPP4-expressing Huh-7 cells (Fig.
206 1A), but it also potently neutralized live MERS-CoV infection of permissive Vero E6 cells by
207 inhibiting the formation of MERS-CoV-induced CPE (Fig. 1B). In addition, Mersmab1 efficiently
208 attenuated the formation of MERS-CoV-induced CPE in permissive Calu-3 cells, confirming its
209 potent anti-MERS-CoV neutralizing activity (Fig. 1C). As a control, an anti-SARS-CoV-RBD
210 mAb, 33G4, did not exhibit any anti-MERS-CoV activities (Fig. 1A, 1B, and 1C) (27).
211 Accordingly, Mersmab1 was chosen for further characterization and evaluation.

212

213 **Mechanism of Mersmab1 in neutralizing MERS-CoV cell entry**

214 To investigate the mechanism of Mersmab1 in neutralizing MERS-CoV cell entry, we
 215 performed RBD/receptor binding assays in the presence of Mersmab1. First, AlphaScreen assay
 216 was carried out by mixing recombinant MERS-CoV RBD-Fc and recombinant DPP4-His₆ in the
 217 presence of Mersmab1-Fab, which is the Fab portion of Mersmab1. The AlphaScreen signal
 218 decreased with increased concentrations of Mersmab1-Fab, indicating that Mersmab1 inhibited
 219 the binding of MERS-CoV RBD to DPP4 in a dose-dependent manner (Fig. 2A). Second, a flow
 220 cytometry assay was performed by incubating MERS-CoV RBD-Fc with DPP4-expressing Huh-7
 221 cells in the presence of Mersmab1. The results show that the binding between MERS-CoV RBD
 222 and DPP4-expressing Huh-7 cells was blocked by Mersmab1 (Fig. 2B), and that the blockade was
 223 also in a dose-dependent manner (Fig. 2C). In contrast, the anti-SARS-CoV mAb 33G4 was
 224 unable to inhibit the binding between MERS-CoV RBD and DPP4-expressing cells (Fig. 2B and
 225 2C). These results suggest that Mersmab1 neutralizes MERS-CoV entry into host cells by
 226 blocking the binding of MERS-CoV RBD to its host receptor, DPP4.

227 To further identify the binding partner for Mersmab1, we measured direct binding interactions
 228 between MERS-CoV RBD and Mersmab1 using both AlphaScreen assay and ELISA.
 229 AlphaScreen assay showed that Mersmab1 specifically bound to MERS-CoV RBD, but not to
 230 SARS-CoV RBD (Fig. 3A). ELISA demonstrated that Mersmab1 specifically bound to
 231 MERS-CoV S1-Fc and RBD-Fc, but not to MERS-CoV S1 N-terminal domain (S-NTD-Fc),
 232 S2-Fc, or hFc (Fig. 3B). As a control, anti-SARS-CoV mAb 33G4 only bound to SARS-CoV
 233 RBD, but not to any of the MERS-CoV spike protein fragments (Fig. 3A and 3B). ELISA also
 234 uncovered that the antibody subtype of Mersmab1 was mainly IgG1 (Fig. 3C). ELISA further
 235 revealed that Mersmab1 lost most of its binding affinity for MERS-CoV S1 or RBD in the
 236 presence of DTT, an agent that disrupts protein disulfide bonds and causes disulfide
 237 bond-stabilized proteins to lose their native conformation. In contrast, an anti-Fc mAb bound the
 238 Fc region of MERS-CoV S1-Fc or RBD-Fc, but did not bind MERS-CoV S1-His without Fc, in
 239 the presence or absence of DTT (Fig. 3D). These results are consistent with the fact that
 240 MERS-CoV RBD contains four pairs of disulfide bond whereas the Fc region contains none, and
 241 hence DTT distorts the native conformation of MERS-CoV RBD, but not that of the Fc region.

242 Taken together, these results suggest that Mersmab1 binds MERS-CoV RBD through recognizing
243 conformational epitopes on the RBD.

244

245 **Mapping neutralizing epitopes in MERS-CoV RBD that are recognized by Mersmab1**

246 Based on the previously determined crystal structure of MERS-CoV RBD in complex with
247 DPP4 (11, 12), we mutated a number of RBD key residues to alanines and then measured how
248 each of these mutations affected the binding of Mersmab1. All of these RBD residues directly
249 contact DPP4; they are L506, D510, R511, E513, D539, W553, and V555. Two other residues,
250 E536 and E565, which do not directly contact DPP4, were also mutated to alanines as controls.
251 Each of the mutant RBD-Fc proteins containing one of the aforementioned mutations was
252 expressed and purified without significant change in its expression levels or solubility (Fig. 4A).
253 This observation indicates that none of these mutations affected the native structure of the RBD,
254 which is consistent with the fact that all of these selected residues are located on the protein
255 surface and not involved in protein folding. ELISA showed that a number of these RBD mutations,
256 including L506A, D510A, R511A, E513A, and W553A, led to significant loss of binding affinity

257 for Mersmab1. Particularly, mutation R511A completely abolished the binding of RBD-Fc to
 258 Mersmab1. In comparison, mutation D539A did not affect the binding between the RBD and
 259 Mersmab1 at all; neither did the two control mutations, E536A and E565A (Fig. 4B). Pseudovirus
 260 entry assay demonstrated that mutation R511A in the MERS-CoV spike protein slightly reduced
 261 pseudovirus entry into target cells, but significantly reduced the inhibitory effect of Mersmab1 on
 262 pseudovirus entry (Fig. 4C and 4D). These results suggest that R511A mutation decreases the
 263 binding affinities of the RBD for DPP4 slightly and for Mersmab1 significantly. Taken together,
 264 these results have identified the neutralizing epitopes in MERS-CoV RBD that are recognized by
 265 Mersmab1.

266 We mapped the recognizing epitopes of Mersmab1 on the determined structural model of
 267 MERS-CoV RBD (12, 15). All of the residues critical for mAb binding are located on the left
 268 ridge of the MERS-CoV receptor-binding motif (RBM) (Fig. 5A), which overlaps with the
 269 DPP4-binding region in MERS-CoV RBD (Fig. 5B). Therefore, the neutralization mechanism of
 270 Mersmab1 is based on the competitive blocking of MERS-CoV RBD binding to DPP4.
 271 Interestingly, these recognizing epitopes appear to differ from the recognizing epitopes of

272 anti-SARS-CoV-RBD mAbs. Currently, three crystal structures are available for SARS-CoV RBD
273 in complex with neutralizing mAbs (36-38). Among the three anti-SARS-CoV mAbs, two bind to
274 the right ridge of the SARS-CoV RBM, whereas one covers the center of the SARS-CoV RBM.
275 Recognizing epitopes of all three anti-SARS-CoV-RBD mAbs overlap with the ACE2-binding
276 region in SARS-CoV RBD. The different recognizing epitopes by anti-MERS-CoV and
277 anti-SARS-CoV mAbs provide a structural basis for studying the antigenicity of different
278 coronavirus RBDs. The identified recognizing epitopes for Mersmab1 can also guide
279 structure-based design of effective anti-MERS-CoV subunit vaccines. Future structure
280 determination of MERS-CoV RBD in complex with Mersmab1 will reveal more detailed
281 knowledge about the neutralizing epitopes in MERS-CoV RBD.

282

283 **DISCUSSION**

284 The newly emerged MERS-CoV poses a continuing threat to human health. The high fatality
285 rate (over 40%) associated with MERS-CoV infections is particularly worrying. Prevention and
286 treatment strategies to control MERS-CoV infection are urgently needed. Although vaccines

287 remain one of the most important approaches against viral infections, they generally take a long
288 time to develop. In addition, vaccines cannot provide immediate prophylactic protection or treat
289 ongoing infections. Instead, the successful clinical application of a therapeutic mAb in preventing
290 and treating RSV infections in infants (26, 39) strongly suggests that therapeutic mAbs can be a
291 promising approach to control MERS-CoV infections in humans.

292 In this study, we identified and characterized a novel monoclonal antibody, Mersmab1, which
293 neutralizes MERS-CoV infection. Mersmab1 inhibits MERS-CoV entry into host cells through
294 binding to the MERS-CoV spike protein RBD and thereby competitively blocks the binding of
295 MERS-CoV RBD to its host receptor, DPP4. The neutralizing epitopes recognized by Mersmab1
296 are located on one edge of the DPP4-binding surface in MERS-CoV RBD. The overlap between
297 these neutralizing epitopes and the DPP4-binding region explains the mechanism by which
298 Mersmab1 potently neutralizes MERS-CoV infection. These results suggest that Mersmab1 can be
299 humanized and serves as a potent passive immunotherapeutic agent for preventing and treating
300 MERS-CoV infections. Like the therapeutic mAb against RSV infection (40, 41), humanized
301 Mersmab1 could be given to patients who are at risk of possible exposure to MERS-CoV and

302 those who are already infected. This approach will be particularly helpful to high-risk populations,
 303 such as immunocompromised people, patients' family members, and healthcare workers.
 304 Therefore, the anti-MERS-CoV neutralizing mAb identified in this study, Mersmab1, provides a
 305 promising approach to combating and controlling the ongoing spread of MERS-CoV in human
 306 populations. In addition, Mersmab1 could be used a tool for studying the conformation and
 307 antigenicity of the MERS-CoV spike protein and for guiding the design of anti-MERS-CoV
 308 vaccines.

309

310 ACKNOWLEDGEMENTS

311 This work was supported by National Program of Infectious Diseases
 312 (2014ZX10004001-004), NIH grant R21AI109094 and intramural fund of the New York Blood
 313 Center (NYB000068) (to L. Du and S. Jiang), NIH grant R01AI089728 (to F. Li), residual funds
 314 and a pilot grant of Center of Biodefense and Emerging Infectious Disease (CBEID), UTMB, (to
 315 C-T. K. Tseng), and the National 973 Basic Research Program of China (2011CB504706).

316

317 **REFERENCES**

- 318 1. **Zaki AM, van BS, Bestebroer TM, Osterhaus AD, Fouchier RA.** 2012. Isolation of a
319 novel coronavirus from a man with pneumonia in Saudi Arabia. *N. Engl. J. Med.*
320 **367**:1814-1820.
- 321 2. **Zhong NS, Zheng BJ, Li YM, Poon, Xie ZH, Chan KH, Li PH, Tan SY, Chang Q, Xie**
322 **JP, Liu XQ, Xu J, Li DX, Yuen KY, Peiris, Guan Y.** 2003. Epidemiology and cause of
323 severe acute respiratory syndrome (SARS) in Guangdong, People's Republic of China, in
324 February, 2003. *Lancet* **362**:1353-1358.
- 325 3. **Skowronski DM, Astell C, Brunham RC, Low DE, Petric M, Roper RL, Talbot PJ,**
326 **Tam T, Babiuk L.** 2005. Severe acute respiratory syndrome (SARS): a year in review.
327 *Annu. Rev. Med.* **56**:357-381.
- 328 4. **Du L, He Y, Zhou Y, Liu S, Zheng BJ, Jiang S.** 2009. The spike protein of SARS-CoV--a
329 target for vaccine and therapeutic development. *Nat. Rev. Microbiol.* **7**:226-236.
- 330 5. **Mailles A, Blanckaert K, Chaud P, van der Werf S, Lina B, Caro V, Campese C,**
331 **Guery B, Prouvost H, Lemaire X, Paty MC, Haeghebaert S, Antoine D, Ettahar N,**

- 332 **Noel H, Behillil S, Hendricx S, Manuguerra JC, Enouf V, La RG, Semaille C, Coignard**
333 **B, Levy-Bruhl D, Weber F, Saura C, Che D.** 2013. First cases of Middle East Respiratory
334 Syndrome Coronavirus (MERS-CoV) infections in France, investigations and implications
335 for the prevention of human-to-human transmission, France, May 2013. *Euro. Surveill* **18**:
336 pii =20502.
- 337 6. **Cauchemez S, Van Kerkhove MD, Riley S, Donnelly CA, Fraser C, Ferguson NM.** 2013.
338 Transmission scenarios for Middle East Respiratory Syndrome Coronavirus (MERS-CoV)
339 and how to tell them apart. *Euro. Surveill* **18**: pii =20503.
- 340 7. **Chan JF, Lau SK, Woo PC.** 2013. The emerging novel Middle East respiratory syndrome
341 coronavirus: the "knowns" and "unknowns". *J. Formos. Med. Assoc.* **112**:372-381.
- 342 8. **Xu Y, Lou Z, Liu Y, Pang H, Tien P, Gao GF, Rao Z.** 2004. Crystal structure of severe
343 acute respiratory syndrome coronavirus spike protein fusion core. *J. Biol. Chem.*
344 **279**:49414-49419.
- 345 9. **Bonavia A, Zelus BD, Wentworth DE, Talbot PJ, Holmes KV.** 2003. Identification of a
346 receptor-binding domain of the spike glycoprotein of human coronavirus HCoV-229E. *J.*

- 347 Virol. **77**:2530-2538.
- 348 10. **Gao J, Lu G, Qi J, Li Y, Wu Y, Deng Y, Geng H, Li H, Wang Q, Xiao H, Tan W, Yan J,**
349 **Gao GF.** 2013. Structure of the fusion core and inhibition of fusion by a heptad-repeat
350 peptide derived from the S protein of MERS-CoV. J. Virol. **87**:13134-13140.
- 351 11. **Wang N, Shi X, Jiang L, Zhang S, Wang D, Tong P, Guo D, Fu L, Cui Y, Liu X,**
352 **Arledge KC, Chen YH, Zhang L, Wang X.** 2013. Structure of MERS-CoV spike
353 receptor-binding domain complexed with human receptor DPP4. Cell Res. **23**:986-993.
- 354 12. **Lu G, Hu Y, Wang Q, Qi J, Gao F, Li Y, Zhang Y, Zhang W, Yuan Y, Bao J, Zhang B,**
355 **Shi Y, Yan J, Gao GF.** 2013. Molecular basis of binding between novel human coronavirus
356 MERS-CoV and its receptor CD26. Nature **500**:227-231.
- 357 13. **Raj VS, Mou H, Smits SL, Dekkers DH, Muller MA, Dijkman R, Muth D, Demmers**
358 **JA, Zaki A, Fouchier RA, Thiel V, Drosten C, Rottier PJ, Osterhaus AD, Bosch BJ,**
359 **Haagmans BL.** 2013. Dipeptidyl peptidase 4 is a functional receptor for the emerging
360 human coronavirus-EMC. Nature **495**:251-254.
- 361 14. **Li W, Moore MJ, Vasilieva N, Sui J, Wong SK, Berne MA, Somasundaran M, Sullivan**

- 362 **JL, Luzuriaga K, Greenough TC, Choe H, Farzan M.** 2003. Angiotensin-converting
363 enzyme 2 is a functional receptor for the SARS coronavirus. *Nature* **426**:450-454.
- 364 15. **Chen Y, Rajashankar KR, Yang Y, Agnihothram SS, Liu C, Lin YL, Baric RS, Li F.**
365 2013. Crystal structure of the receptor-binding domain from newly emerged Middle East
366 respiratory syndrome coronavirus. *J. Virol.* **87**:10777-10783.
- 367 16. **Li F, Li W, Farzan M, Harrison SC.** 2005. Structure of SARS coronavirus spike
368 receptor-binding domain complexed with receptor. *Science* **309**:1864-1868.
- 369 17. **Li F.** 2013. Receptor recognition and cross-species infections of SARS coronavirus.
370 *Antiviral Res.* **100**:246-254.
- 371 18. **Li F.** 2012. Evidence for a common evolutionary origin of coronavirus spike protein
372 receptor-binding subunits. *J. Virol.* **86**:2856-2858.
- 373 19. **Lu L, Liu Q, Zhu Y, Chan KH, Qin L, Li Y, Wang Q, Chan JF, Du L, Yu F, Ma C, Ye**
374 **S, Yuen KY, Zhang R, Jiang S.** 2014. Structure-based discovery of Middle East respiratory
375 syndrome coronavirus fusion inhibitor. *Nat. Commun.* **5**:3067.
- 376 20. **Berzofsky JA, Ahlers JD, Janik J, Morris J, Oh S, Terabe M, Belyakov IM.** 2004.

- 377 Progress on new vaccine strategies against chronic viral infections. *J. Clin. Invest.*
378 **114**:450-462.
- 379 21. **Du L, Zhao G, Chan CC, Sun S, Chen M, Liu Z, Guo H, He Y, Zhou Y, Zheng BJ,**
380 **Jiang S.** 2009. Recombinant receptor-binding domain of SARS-CoV spike protein
381 expressed in mammalian, insect and *E. coli* cells elicits potent neutralizing antibody and
382 protective immunity. *Virology* **393**:144-150.
- 383 22. **Du L, Kou Z, Ma C, Tao X, Wang L, Zhao G, Chen Y, Yu F, Tseng CT, Zhou Y, Jiang**
384 **S.** 2013. A truncated receptor-binding domain of MERS-CoV spike protein potently inhibits
385 MERS-CoV infection and induces strong neutralizing antibody responses: implication for
386 developing therapeutics and vaccines. *PLoS One.* **8**:e81587.
- 387 23. **He Y, Zhou Y, Liu S, Kou Z, Li W, Farzan M, Jiang S.** 2004. Receptor-binding domain
388 of SARS-CoV spike protein induces highly potent neutralizing antibodies: implication for
389 developing subunit vaccine. *Biochem. Biophys. Res. Commun.* **324**:773-781.
- 390 24. **Du L, Jin L, Zhao G, Sun S, Li J, Yu H, Li Y, Zheng BJ, Liddington RC, Zhou Y,**
391 **Jiang S.** 2013. Identification and structural characterization of a broadly neutralizing

- 392 antibody targeting a novel conserved epitope on the influenza virus H5N1 hemagglutinin. J.
393 Virol. **87**:2215-2225.
- 394 25. **Zhu X, Guo YH, Jiang T, Wang YD, Chan KH, Li XF, Yu W, McBride R, Paulson JC,**
395 **Yuen KY, Qin CF, Che XY, Wilson IA.** 2013. A unique and conserved neutralization
396 epitope in H5N1 influenza viruses identified by an antibody against the
397 A/Goose/Guangdong/1/96 hemagglutinin. J. Virol. **87**:12619-12635.
- 398 26. **Fenton C, Scott LJ, Plosker GL.** 2004. Palivizumab: a review of its use as prophylaxis for
399 serious respiratory syncytial virus infection. Paediatr. Drugs **6**:177-197.
- 400 27. **He Y, Lu H, Siddiqui P, Zhou Y, Jiang S.** 2005. Receptor-binding domain of severe acute
401 respiratory syndrome coronavirus spike protein contains multiple conformation-dependent
402 epitopes that induce highly potent neutralizing antibodies. J. Immunol. **174**:4908-4915.
- 403 28. **Sui J, Hwang WC, Perez S, Wei G, Aird D, Chen LM, Santelli E, Stec B, Cadwell G,**
404 **Ali M, Wan H, Murakami A, Yammanuru A, Han T, Cox NJ, Bankston LA, Donis RO,**
405 **Liddington RC, Marasco WA.** 2009. Structural and functional bases for broad-spectrum
406 neutralization of avian and human influenza A viruses. Nat. Struct. Mol. Biol. **16**:265-273.

- 407 29. Corti D, Voss J, Gamblin SJ, Codoni G, Macagno A, Jarrossay D, Vachieri SG, Pinna
408 D, Minola A, Vanzetta F, Silacci C, Fernandez-Rodriguez BM, Agatic G, Bianchi S,
409 Giacchetto-Sasselli I, Calder L, Sallusto F, Collins P, Haire LF, Temperton N,
410 Langedijk JP, Skehel JJ, Lanzavecchia A. 2011. A neutralizing antibody selected from
411 plasma cells that binds to group 1 and group 2 influenza A hemagglutinins. Science
412 333:850-856.
- 413 30. Whittle JR, Zhang R, Khurana S, King LR, Manischewitz J, Golding H, Dormitzer PR,
414 Haynes BF, Walter EB, Moody MA, Kepler TB, Liao HX, Harrison SC. 2011. Broadly
415 neutralizing human antibody that recognizes the receptor-binding pocket of influenza virus
416 hemagglutinin. Proc. Natl. Acad. Sci. U. S. A 108:14216-14221.
- 417 31. Du L, Zhao G, Sun S, Zhang X, Zhou X, Guo Y, Li Y, Zhou Y, Jiang S. 2013. A critical
418 HA1 neutralizing domain of H5N1influenza in an optimal conformation induces strong
419 cross-protection. PLoS. One 8:e53568.
- 420 32. Du L, Zhao G, Kou Z, Ma C, Sun S, Poon VK, Lu L, Wang L, Debnath AK, Zheng BJ,
421 Zhou Y, Jiang S. 2013. Identification of a receptor-binding domain in the S protein of the

- 422 novel human coronavirus Middle East respiratory syndrome coronavirus as an essential
- 423 target for vaccine development. J. Virol. **87**:9939-9942.
- 424 33. **Zhao G, Du L, Ma C, Li Y, Li L, Poon VK, Wang L, Yu F, Zheng BJ, Jiang S, Zhou Y.**
- 425 2013. A safe and convenient pseudovirus-based inhibition assay to detect neutralizing
- 426 antibodies and screen for viral entry inhibitors against the novel human coronavirus
- 427 MERS-CoV. Virol. J. **10**:266.
- 428 34. **Tao X, Hill TE, Morimoto C, Peters CJ, Ksiazek TG, Tseng CT.** 2013. Bilateral entry
- 429 and release of Middle East respiratory syndrome coronavirus induces profound apoptosis of
- 430 human bronchial epithelial cells. J. Virol. **87**:9953-9958.
- 431 35. **Tao X, Hill TE, Lewis J.** 2013. Evaluation of different glutathione S-transferase-tagged
- 432 protein captures for screening E6/E6AP interaction inhibitors using AlphaScreen. J. Virol.
- 433 **87**:560-567.
- 434 36. **Prabakaran P, Gan J, Feng Y, Zhu Z, Choudhry V, Xiao X, Ji X, Dimitrov DS.** 2006.
- 435 Structure of severe acute respiratory syndrome coronavirus receptor-binding domain
- 436 complexed with neutralizing antibody. J. Biol. Chem. **281**:15829-15836.

- 437 37. **Pak JE, Sharon C, Satkunarajah M, Auperin TC, Cameron CM, Kelvin DJ,**
438 **Seetharaman J, Cochrane A, Plummer FA, Berry JD, Rini JM.** 2009. Structural insights
439 into immune recognition of the severe acute respiratory syndrome coronavirus S protein
440 receptor binding domain. *J. Mol. Biol.* **388**:815-823.
- 441 38. **Hwang WC, Lin Y, Santelli E, Sui J, Jaroszewski L, Stec B, Farzan M, Marasco WA,**
442 **Liddington RC.** 2006. Structural basis of neutralization by a human anti-severe acute
443 respiratory syndrome spike protein antibody, 80R. *J. Biol. Chem.* **281**:34610-34616.
- 444 39. **Wu SY, Bonaparte J, Pyati S.** 2004. Palivizumab use in very premature infants in the
445 neonatal intensive care unit. *Pediatrics* **114**:e554-e556.
- 446 40. **Groothuis JR, Nishida H.** 2002. Prevention of respiratory syncytial virus infections in
447 high-risk infants by monoclonal antibody (palivizumab). *Pediatr. Int.* **44**:235-241.
- 448 41. **Pollack P, Groothuis JR.** 2002. Development and use of palivizumab (Synagis): a passive
449 immunoprophylactic agent for RSV. *J. Infect. Chemother.* **8**:201-206.
- 450
- 451

452 **FIGURE LEGEND**

453 **FIG 1** Mersmab1 inhibited MERS-CoV-spike-mediated pseudovirus entry into DPP4-expressing
 454 Huh-7 cells and neutralized MERS-CoV infection in both Vero E6 and Calu-3 cells.
 455 Anti-SARS-CoV-RBD mAb, 33G4, was included as a control. (A) Selected anti-MERS-CoV
 456 mAbs (Mersmab1, Mersmab2, Mersmab3, and Mersmab10) were tested for their inhibition of
 457 MERS-CoV-spike-mediated pseudovirus entry into DPP4-expressing Huh-7 cells. The data are
 458 presented as mean percentages of inhibition \pm standard deviation (SD) (n=4). (B)
 459 Anti-MERS-CoV mAbs were tested for their neutralizing activity against infection by authentic
 460 MERS-CoV (EMC strain) in Vero E6 cells. The neutralization capability of mAbs was
 461 characterized using 50% neutralization dose (ND₅₀), which was defined as the concentration of the
 462 mAb that reduced CPE by 50%. The data are presented as mean ND₅₀ \pm SD (n=3). (C) Mersmab1
 463 neutralized MERS-CoV infection in Calu-3 cells. A standard micro-neutralization assay was used
 464 to assess the potency of Mersmab1 in neutralizing MERS-CoV infection. Levels of CPE were
 465 scored as follows: CPE0 (no CPE), CPE1 (5–10%), CPE2 (10–25%), CPE3 (25–50%), and CPE4
 466 (>50%).

467

468 **FIG 2** Mersmab1 blocked the binding between MERS-CoV RBD and its receptor DPP4. (A)

469 AlphaScreen assay was performed to detect whether Mersmab1 could block the binding between

470 recombinant MERS-CoV RBD and recombinant DPP4. MERS-CoV RBD-Fc (0.01 µg/ml) was

471 mixed with DPP4-His₆ (0.27 µg/ml) in the presence of Mersmab1-Fab. (B) Flow cytometry assay

472 was carried out to detect whether Mersmab1 could block the binding between MERS-CoV RBD

473 and host cells expressing DPP4 on their surface. Grey shade, Huh-7 cell control; Red line, binding

474 of MERS-CoV RBD-Fc (MERS RBD, 0.5 µg/ml) to Huh-7 cells; Blue line, Mersmab1 inhibits

475 MERS RBD (0.5 µg/ml) binding Huh-7 cells; Green line, anti-SARS-CoV mAb 33G4 (0.5 µg/ml)

476 control. (C) Flow cytometry assay showed that Mersmab1 inhibited the binding between

477 MERS-CoV RBD and DPP4 in a dose-dependent fashion. The data in (A) and (C) are presented

478 as mean ± SD (n=4), and in (C) as percentage of inhibition (%).

479

480 **FIG 3** Mersmab1 recognizes MERS-CoV spike protein RBD in a conformation-dependent

481 manner. (A) AlphaScreen assay was performed to detect the binding between Mersmab1 and

482 MERS-CoV RBD. MERS-CoV RBD-His₆ (2.8 µg/ml) was mixed with Mersmab1 (0.5 µg/ml).

483 SARS-CoV 33G4 mAb and SARS-CoV RBD protein were used as controls. (B) ELISA was
 484 carried out to detect the binding between Mersmab1 (containing mouse IgG Fc) and MERS-CoV
 485 spike protein fragments (containing human IgG Fc). Recombinant human Fc (hFc), SARS-CoV
 486 RBD, and anti-SARS-CoV mAb 33G4 were used as controls. (C) ELISA was performed to
 487 identify Mersmab1 IgG subtypes using antibodies that target mouse IgG1, IgG2a, IgG2b, and
 488 IgG3, respectively. (D) ELISA was used to detect the binding between Mersmab1 and
 489 MERS-CoV S1 protein fragments in the presence or absence of DTT. An anti-Fc mAb (Sigma)
 490 was used as the control. All data are presented as mean \pm SD (n=4).

491

492 **FIG 4** Mapping of recognizing epitopes of Mersmab1 in MERS-CoV RBD. (A) Expression levels
 493 of mutant MERS-CoV RBDs in 293T cell culture supernatant were detected using SDS-PAGE
 494 (stained by Coomassie blue) (top) and Western blot (recognized by anti-MERS-CoV-S1
 495 polyclonal antibodies) (bottom). The protein molecular weight marker (kDa) is indicated on the
 496 left. (B) ELISA was performed to detect the binding of Mersmab1 to mutant MERS-CoV RBD
 497 proteins. (C) Mutation R511A in the MERS-CoV spike protein slightly reduced
 498 MERS-CoV-spike-mediated pseudovirus entry into DPP4-expressing Huh-7 cells. (D) R511A

499 mutation in the MERS-CoV spike protein significantly reduced the inhibitory effect of Mersmab1
 500 on MERS-CoV-spike-mediated pseudovirus entry. All data are presented as mean \pm SD (n=2).
 501 MERS-CoV RBD protein wildtype was used as the control for (A) and (B), while pseudovirus
 502 wildtype was included as the control for (C) and (D).

503

504 **FIG 5** Structural analysis of the recognizing epitopes of anti-MERS-CoV-RBD and
 505 anti-SARS-CoV-RBD mAbs. (A) Crystal structure of MERS-CoV RBD. Core structure is in cyan,
 506 and RBM is in pink. Critical residues at the RBD-DPP4 binding interface are in green (PDB ID:
 507 4KQZ). (B) Crystal structure of MERS-CoV RBD (cyan) complexed with its receptor, human
 508 DPP4 (in yellow) (PDB ID: 4KR0). (C) Crystal structure of SARS-CoV RBD complexed with
 509 anti-SARS-CoV mAb m396 Fab (PDB ID: 2DD8). The light chain and heavy chain of the mAb
 510 are in yellow and green, respectively. (D) Crystal structure of SARS-CoV RBD complexed with
 511 anti-SARS-CoV mAb F26G19 Fab (PDB ID: 3BGF). (E) Crystal structure of SARS-CoV RBD
 512 complexed with anti-SARS-CoV mAb 80R scFv (PDB ID: 2GHW).

513

514

Fig. 1

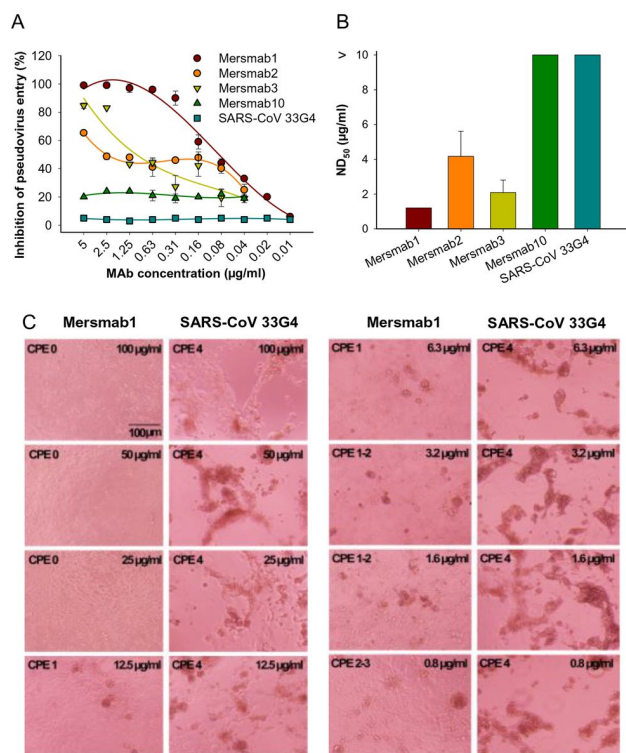


Fig. 2

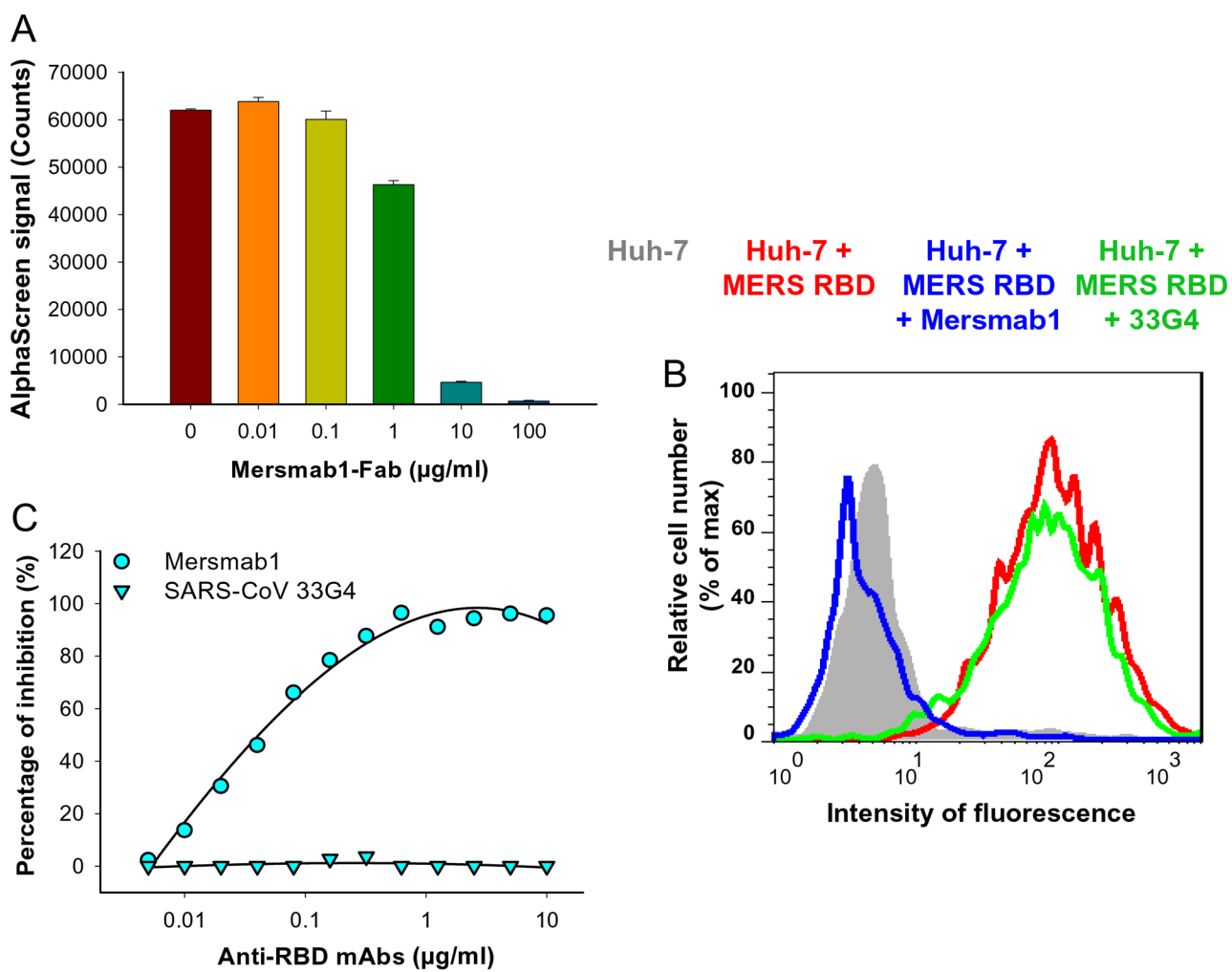


Fig. 3

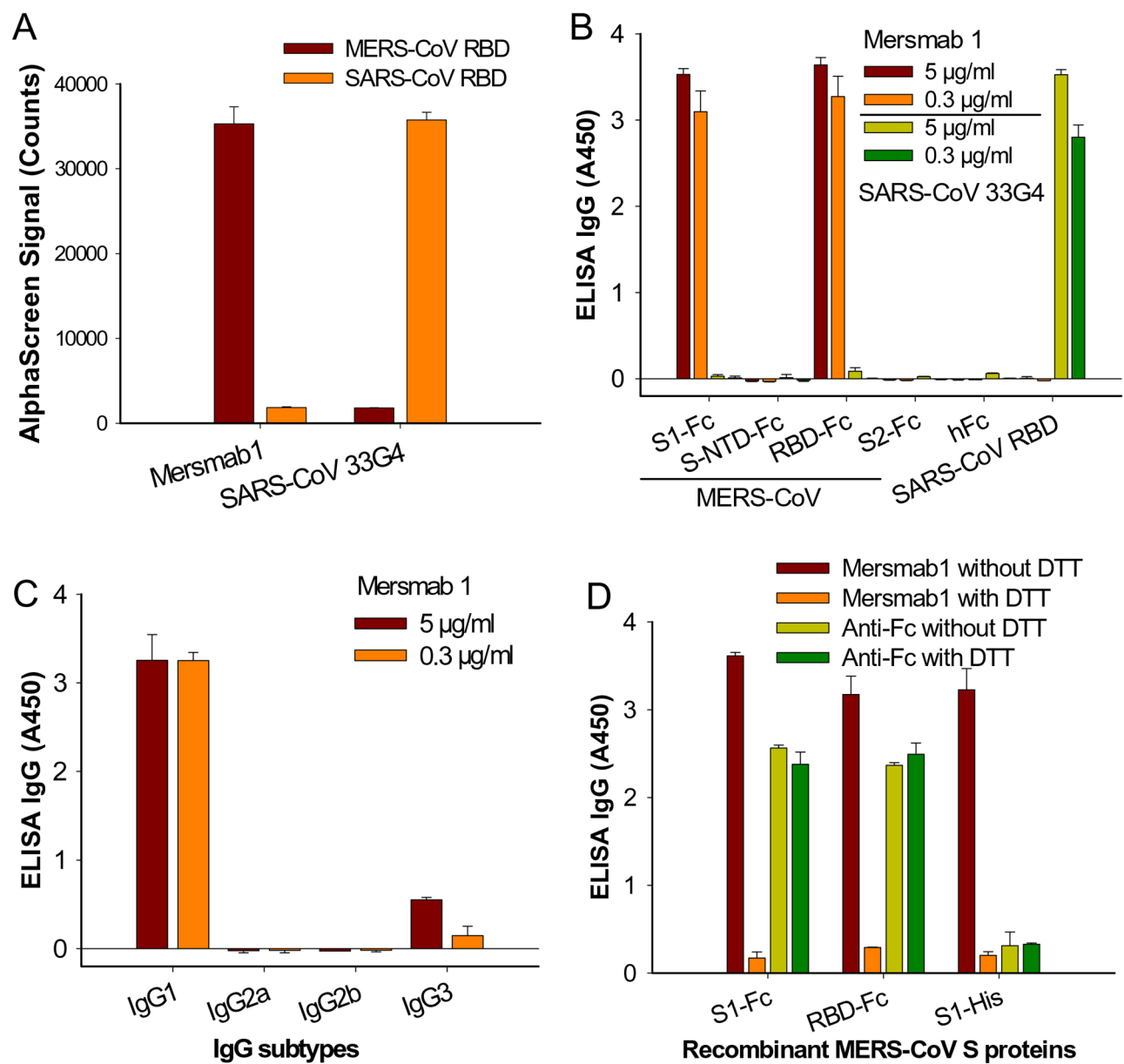


Fig. 4

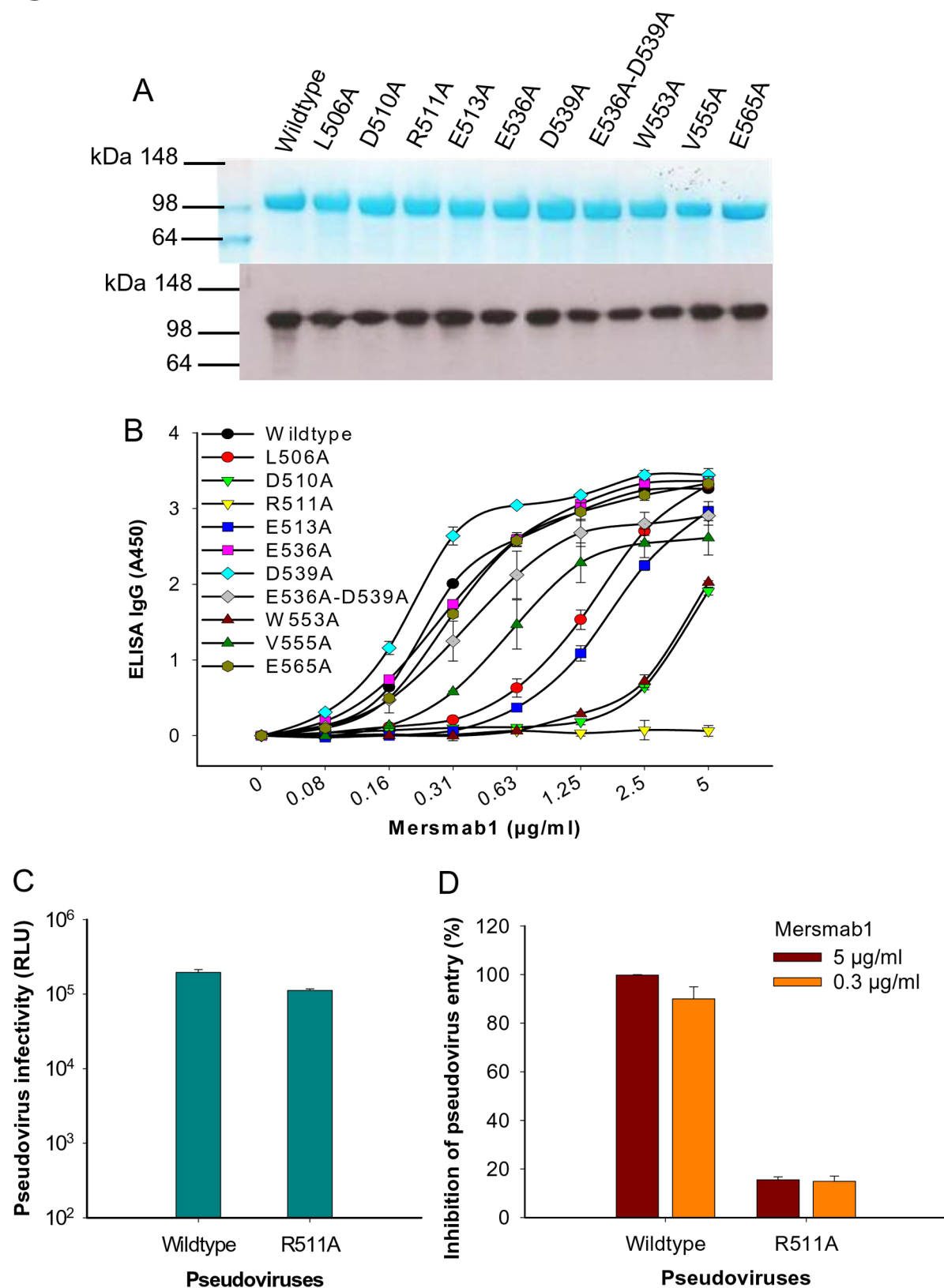


Fig. 5

